Dynamics and thermodynamics of a nickel uptake from a water system onto the blast furnace sludge

Rađenović, Ankica; Medunić, Gordana

Permanent link / Trajna poveznica: https://urn.nsk.hr/urn:nbn:hr:115:627157

Download date / Datum preuzimanja: **2024-05-20**

DYNAMICS AND THERMODYNAMICS OF A NICKEL UPTAKE
FROM A WATER SYSTEM ONTO THE BLAST FURNACE SLUDGE

Ankica Radjenovic[1], Gordana Medunic[2]

[1]*University of Zagreb, Faculty of Metallurgy*
 Aleja narodnih heroja 3, 44000 Sisak, Croatia
 E-mail: radenova@simet.hr
[2]*University of Zagreb, Faculty of Science, Department of Geology, Zagreb, Croatia*

ABSTRACT

This study describes the use of blast furnace sludge (BFS) for the removal of toxic Ni(II) ions from a water system. Blast furnace sludge is a by-product and a waste material of the steelmaking industry. Chemical and mineralogical characteristics of BFS are determined by Proton Induced X-ray Emission and X-ray Diffraction methods. The surface area properties are determined by the Brunauer-Emmett-Teller method. The adsorption is investigated in a batch adsorption system in view of its kinetics and thermodynamics. The kinetic experiments show that the adsorption process follows a pseudo-second order model. The adsorption mechanism is investigated by intra-particle diffusion and Boyd-Reichenberg kinetic models. Thermodynamic parameters (activation free energy change, activation enthalpy change, and activation entropy change) reveal that the adsorption of Ni(II) on BFS is spontaneous, exothermic, and chemical in nature. The results suggest that BFS is an inexpensive and efficient adsorbent for the removal of Ni(II) ions from aqueous solutions.
 Keywords: metallurgical waste, blast furnace sludge, Ni(II) adsorption, kinetics, thermodynamics.

INTRODUCTION

The rapid industrialization has seriously contributed to the release of toxic heavy metals to water and wastewater. Activities such as petroleum refining, tanning, agricultural activities, mining, paint manufacturing, electroplating, battery manufacturing, chemical production and metal processing can introduce toxic substances in form of heavy metal contamination. Metals such as lead, cadmium, copper, arsenic, nickel, chromium, zinc and mercury have been recognized as hazardous heavy metals. Unlike organic wastes, heavy metals are non-biodegradable and they can be accumulated in the living tissues causing various diseases and disorders; therefore they must be removed prior to their discharge [1, 2]. The main source of nickel pollution of water refers to the industrial production processes such as galvanization, smelting, mining, batteries manufac-

turing and metal finishing. The health effects of nickel include higher chances of the development of lung, nose, larynx and respiratory failure as well as birth defects. Certain compounds of nickel have been listed as carcinogenic [3].

Adsorption, among the various accessible water treatment technologies, is considered preferable due to its convenience, ease of operation and simplicity of design. Furthermore, this process can remove/minimize different types of pollutants and which is why it has a wide applicability in water pollution control [4].

Industrial waste is also one of the potentially low-cost adsorbent for the removal of heavy metals from water/wastewaters. Generally, industrial wastes are generated as by-products. Since these materials are locally available in large quantities, they are inexpensive. Various types of industrial wastes such as fly ash, iron and steelmaking slags, blast furnace sludge, waste slurry,

lignin, iron (III) hydroxide, carbon anode dust and red mud have been explored for their technical feasibility for the removal of toxic heavy metals from contaminated water [1, 5 - 7]. If the solid wastes could be used as low-cost adsorbents, they will provide a two-fold advantage in respect to the environmental protection. Firstly, the waste materials volume could be partly decreased, and secondly - the low-cost adsorbent can reduce the wastewaters pollution at a reasonable cost [8].

Blast furnace sludge (BFS) is a by-product of the steelmaking industry. The gases generated during the manufacture of pig iron carry a dust load which is cleaned prior to its release in the atmosphere. The coarse particles in the exhaust gases are removed by passing the gases through a large lined chamber. The velocity of gases is reduced to allow the settling of the dust load and the waste material is collected as a blast-furnace dust. The finer particles, which remain in the gas, are removed in wet scrubbers; the waste material collected here is BFS [9].

This paper presents the research of Ni(II) ions uptake using BFS as a potential inexpensive adsorbent in a polluted water treatment system. The important factor in the adsorption systems design refers to the prediction of the adsorption dynamics and thermodynamics.

EXPERIMENTAL

Blast furnace sludge sample

A BFS sample was collected from the Croatian iron and steelmaking factory. The mass of 5 kg was homogenized manually. For the analysis, a representative sample of BFS was obtained by a quartering technique. It was dried at 105°C for 4 h and sieved to particle size ≤ 56 μm. The chemical composition of the grounded sample was determined by Proton Induced X-ray Emission (PIXE) and Rutherford Backscattering Spetrometry (RBS) techniques. Mineral phase composition was determined by X-ray diffraction (XRD) analysis using a Philips PW 1710 diffractometer with CuK$_\alpha$ radiation. The surface area properties were determined by the Brunauer-Emmett-Teller (BET) method using Micromeritics ASAP 2000 adsorption instrument.

Adsorption experiment

The adsorption of nickel ions from an aqueous solution on BFS was performed using a batch technique. A standard solution containing 1000 mg/L of Ni(II) was prepared by dissolving NiCl$_2$×6H$_2$O with deionized water. Different initial concentrations of Ni(II) solutions were prepared by the dilution of 1000 mg/L Ni standard solution.

For each experiment, 50 ml of the nickel solution of a known concentration (ranging from 100 mg/L to 500 mg/L) and a known amount of the adsorbent (0.325 g) were placed in a 100 ml conical flask. This mixture was agitated in a temperature-controlled shaker at a constant speed of 60 rpm for 2.5 h. Although the experiments were performed within the time intervals from 0 h - 48 h, the equilibrium was established within 24 h. The adsorption kinetics was determined by analyzing the adsorptive uptake of the nickel ions from the aqueous solution at different time intervals. The temperature effect on the adsorption characteristics was investigated by determining the adsorption at 293 K, 313 K and 333 K. The suspension obtained in the course of the reaction was filtered after its completion using Whatman filter paper No. 44. The supernatant was analyzed spectrophotometrically for Ni(II) concentration at pH of 7.8 following the standard method of water and wastewater examination [10]. The uptake values were determined as a difference between the initial Ni(II) concentration, and the one in the supernatant.

The experiments were run in triplicate under identical conditions to check the analytical reproducibility during the concentration measurements and the average values were reported.

RESULTS AND DISCUSSION
Characterization of BFS sample

The results of chemical composition showed that BFS is dominated by O (42.23 %) and C (31.74 %), followed by Si (6 %), Zn (4.52 %), Na (3 %), Al (3 %), Fe (2,9 %), Ca (2,3 %), Mg (1 %), Pb (0,99 %), K (0,66 %), Mn (0,66 %), S (0,62 %), P (0,14 %), Cl (0,05 %), Ti (0,05%), Cu (0,01%), etc. The mineralogical inventory revealed that BFS is dominated by amorphous phase (76.2%) composed mainly of the coke and less crystalline oxides, carbonates or hydroxides of metals: CaCO$_3$, Fe$_3$O$_4$, Al$_2$Si$_2$O$_5$(OH)$_4$, ZnCO$_3$, Ca,Mg (CO$_3$), α –SiO$_2$, α –Fe$_2$O$_3$, and α –Fe).

The fundamentally significant feature of the adsorbents refers to their high porosity and usually high surface area. That is why their most important characteri-

Table 1. Kinetic model parameters for the Ni(II) adsorption onto the BFS.

Kinetic model	Initial concentration	Parameter	Value
	150 mg/L	k_1, 1/h	
		$q_{e(theor.)}$= 0.5266 mg/g	0.1693
		$q_{e(exp.)}$= 13.7170 mg/g	
Pseudo- first order		R^2	
	350 mg/L	k_1, 1/h	0.6341
		$q_{e(theor.)}$= 0.6540 mg/g	0.1106
		$q_{e(exp.)}$= 36.6030 mg/g	
		R^2	
	150 mg/L	k_2, g/mgh	0.2723
		$q_{e(theor.)}$= 14.245mg/g	0.0496
		$q_{e(exp.)}$= 13.717 mg/g	
Pseudo- second order		R^2	
	350 mg/L	k_2,g/mgh	0.9970
		$q_{e(theor.)}$=37.3134mg/g	0.0279
		$q_{e(exp.)}$= 36.6030 mg/g	
		R^2	
	150 mg/L	k_{id}, mg/gh$^{1/2}$	0.9980
Weber-Morris		R^2	1.7237
		C	0.7090
	350 mg/L	k_{id}, mg/gh$^{1/2}$	4,7674
		R^2	4.6574
		C	0.6830
			13.083

stics deal with total pore volumes, pore size distribution over the pore diameter and the specific surface area. The adsorption capacities can be related to the surface area properties of BFS. The value of BET surface area, S_p, is equal to 31.46 m^2/g. It could be explained by the fine – grained particle size of BFS and its porous nature. The total pore volume (1.7 nm - 300 nm) is calculated at the relative pressure close to saturation in the adsorption branch yielding $V_p = 157 \cdot 10^{-3}$ cm^2/g. The average pore diameter, d, amount to 17.88 nm. According to

the International Union of Pure and Applied Chemistry (IUPAC) classification, the pores of the porous material are classified in three groups: micropores (width d < 2 nm), mesopores (2 nm < d < 50 nm) and macropores (d > 50 nm) [11]. Hence, BFS may be considered a mesoporous material.

Adsorption dynamics

It is known that the adsorption dynamics is useful for the description of the solute uptake rate which controls the residence time of the adsorbate at the solid-solution interface. There are essentially three consecutive steps of adsorption of materials from a solution by porous adsorbents such as BFS. The first of these is the bulk diffusion which usually happens at a faster rate. The other two are outer diffusion (film diffusion) and pore diffusion. The slowest of these two limits essentially the adsorption rate [12, 13].

In order to establish the mechanism of the sorption process and the potential rate controlling step, the experimental data are tested using two types of kinetic models, namely reaction-based and diffusion based models [14].

A kinetic study

Fig. 1 shows the effect of the equilibrium time on the adsorption rate of Ni (II) on BFS. It is observed that the amount of the adsorbed nickel ions increases with the increase of the initial concentration and the contact time. Fig. 1 shows that the rate of Ni(II) uptake is very rapid for the initial contact period of 4 h. Thereafter, the nickel uptake process proceeds at a very slow rate, and finally reaches saturation. The saturation time is found

to be 24 h irrespective of the initial Ni (II) concentration.

The widely used kinetic models employed to explain solid/liquid adsorption as a chemical reaction refer to the pseudo-first order kinetic model (Lagergren model) and the pseudo-second order kinetic model (Ho model) expressed by following simplified linear equations [15, 16]:

A pseudo-first order kinetic model:

$$ln(q_e\text{-}q_t) = lnq_e - k_1 \cdot t \qquad (1)$$

A pseudo-second order kinetic model:

$$\frac{t}{q_t} = \frac{1}{k_2 \cdot q_e^2} + \frac{t}{q_e} \qquad (2)$$

where q_e is the equilibrium adsorption capacity (mg/g), q_t is the amount of nickel ions adsorbed at any time t (mg/g), t is the time (h), k_1 is the rate constant of the pseudo-first order adsorption (1/h), while k_2 is the rate constant of the pseudo-second order adsorption (g/mgh).

For many adsorption processes, the pseudo-first order kinetics is found adequate only for the initial 20 min to 30 min of the interaction time but not for the whole contact time range. Parameters k_1 and q_e can be evaluated from the graph of ln (q_e-q_t) versus t (Fig. 2). If a straight line is obtained, then the adsorption follows a pseudo first order kinetics model. The values of $q_{e, exp}$, k_1, the theoretic values $q_{e,(theor)}$, and the correlation coefficient R^2 are all listed in Table 1. It can be seen that the correlation coefficients are not high, while the agreement between $q_{e,(theor)}$ and $q_{e, exp}$ is also not satisfying.
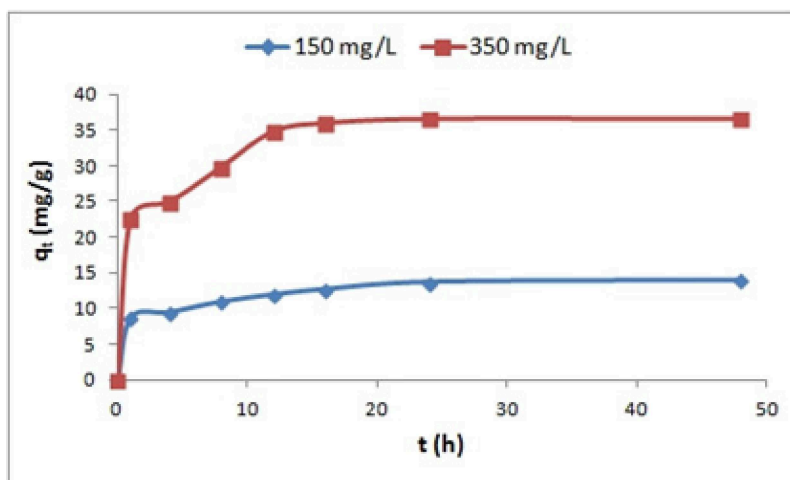
If the adsorption system follows a pseudo-second

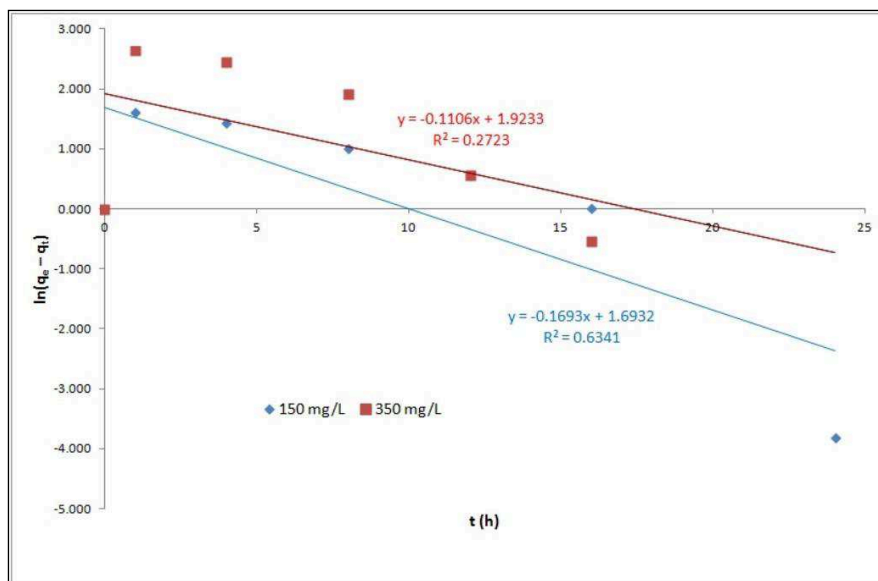Fig. 1. Adsorption kinetics for the adsorption of Ni(II) ions onto the BFS.

Fig. 2. Pseudo-first order plot of Ni(II) adsorption kinetics onto the BFS.

order kinetics, then the rate limiting step may refer to the chemical adsorption which involves valency forces through sharing or exchange of electrons between the adsorbent and the adsorbate. Then a plot of t/q_t versus t should be linear and k_2 and q_e can be determined from the intercept and the slope of the graph (Fig. 3). The correlation coefficient (R^2) values of the linear plots (Fig. 3), obtained on the ground of the pseudo-second order model, are very close to 1 (0.9970 and 0.9980, Table 1). The theoretical and the experimental q_e values show the best agreement. Hence, it can be concluded that the adsorption of Ni(II) ions

on BFS proceeds in accordance with a pseudo-second order kinetic model.

Adsorption mechanism

In order to establish the mechanism of the sorption process and the potential rate controlling step, the experimental data are tested using two types of kinetic models, namely reaction-based and diffusion-based models [14]. Along with the adsorption on the outer surface of the adsorbents, there is also a possibility of intraparticle diffusion from the outer surface into the pores of the
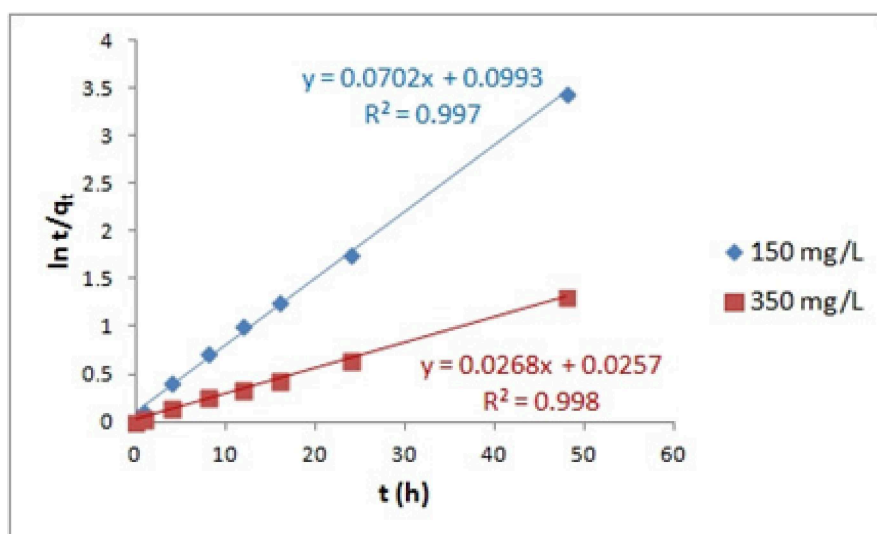

Fig. 3. Pseudo-second order plot of Ni(II) adsorption kinetics onto the BFS.
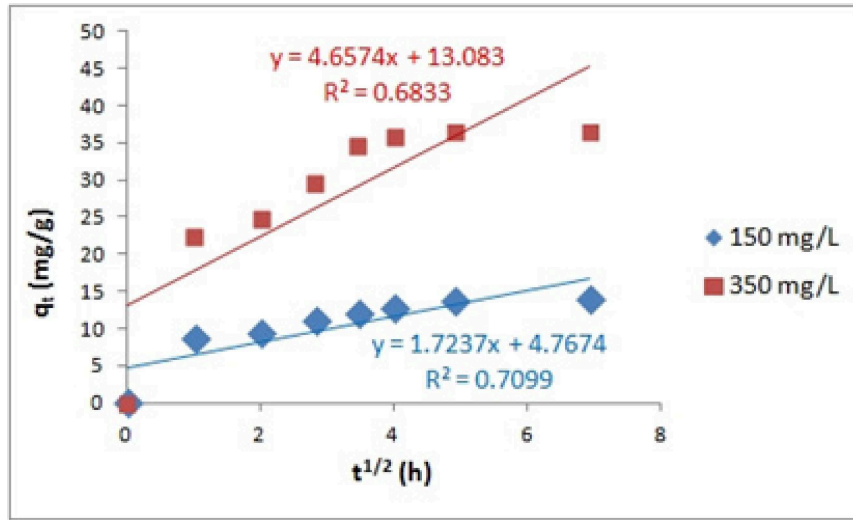
Fig. 4. Intraparticle-diffusion plot of Ni(II) adsorption kinetics onto the BFS.

material. The intra-particle diffusion (Weber-Morris) is described by the equation [17]:

$$q_{t} = k_{id}.t^{1/2} + C \qquad (3)$$

where C is the intercept, while k_{id} is the intraparticle diffusion rate constant (mg/g h$^{1/2}$).

The plot q_t versus t$^{1/2}$ should be linear according to this model implicating that the intraparticle diffusion is involved in the adsorption process. If these lines pass through the origin, then the intraparticle diffusion is the rate-controlling step [18]. If the plots do not pass through the origin (C is not zero), the intraparticle diffusion is not the only rate-limiting step, and some other kinetic models can simultaneously describe the adsorption rate. The rate parameter for the intraparticle diffusion, k_{id}, can be calculated from the slope of the linear plot. The intercept value C gives information about the thickness of the boundary layer. The larger the intercept, the greater the boundary layer effect is [19, 20]. The values of k_d (mg/gh$^{1/2}$) referring to Ni(II) adsorption on BFS are estimated from the slope of the plot of q(mg/g) versus $t^{1/2}$ (Fig. 4). The values of k_{id} and C are presented in Table 1.

As can be seen from Fig. 4, the plot q_t versus t$^{1/2}$ is not quite linear, and does not pass through the origin; this means that the intraparticle diffusion is not the only rate-limiting step. An additional confirmation of these results is obtained using the Boyd-Reichenberg kinetic model [21, 22] described by the following equation:

$$F = 1 - (\frac{6}{\pi^2}) \exp(-B_t) \qquad (4)$$

where F is the fractional attainment of equilibrium at time t $(F = q_t/q_e)$, while B_t is a mathematical function of F. Considering that q_t and q_e are the adsorbate adsorption quantities at time t and at equilibrium, respectively, Eq. (4) can be rearranged into the following form:

$$B_t = -0.4977 - \ln(1-F) \qquad (5)$$

$$B_t = 6.28318 - 3.2899F - 6.28318(1-1.0470F)^{1/2} \qquad (6)$$

The value of B_t is obtained by applying either Eq. (5) when F (t) > 0.85 or Eq. (6) when F (t) ≤ 0.85.

As shown in Fig. 5, plots $B_t - t$ display linear profiles, but do not pass through the origin. These results indicate that the film-diffusion controls the adsorption rate at the beginning of the adsorption, while other mechanisms such as intra-particle diffusion take over and control subsequently the adsorption rate.

An adsorption thermodynamics study

The type of the adsorption nature, physical or chemical, can be evaluated by calculating the activation energy and the thermodynamic parameters. The rate constant of the saturation type of the adsorption reaction (k_1 or k_2) is expressed as a function of the temperature [23] by the Arrhenius equation (Eq. 7):
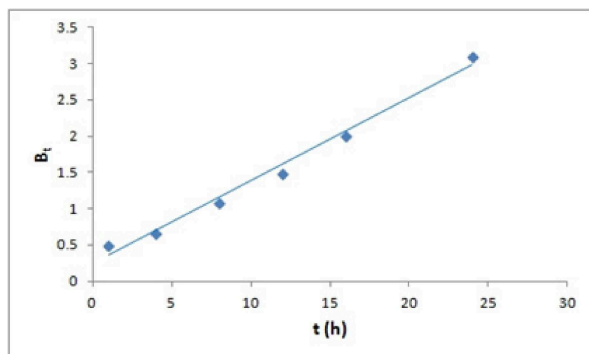
$$k = A \exp(-E_a / RT) \qquad (7)$$

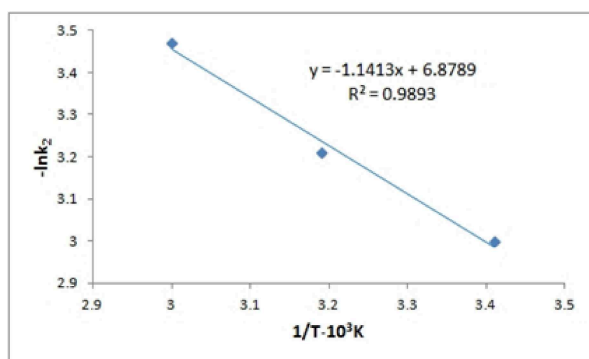Fig. 5. Boyd- Reichenberg plot for Ni(II) adsorption onto the BFS.
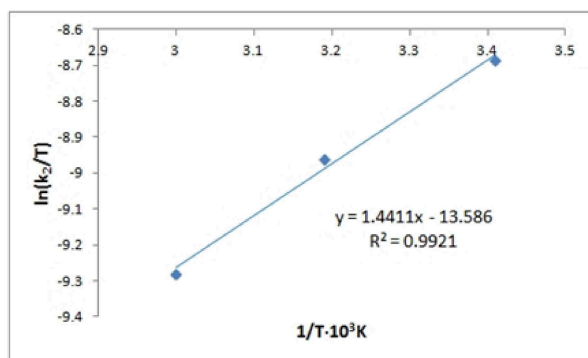

Fig. 6. Arrhenius plot.

Fig. 7. Plot of $ln(k_2/T)$ *vs*.1/T.

where k is the rate constant, A is the frequency factor, E_a is the activation energy of the process (kJ/mol), R is the universal gas constant (J/mol K), while T is the temperature (K). The ln k_2 values are plotted against $1/T$ (Fig. 6), and the activation energy is found equal to 9.49 kJ/mol. The activation energy of physical adsorption is usually

no more than 4.2 kJ/mol, since the forces involved are weak. The chemical adsorption is specific and involves much stronger forces. Two types of chemical adsorption are encountered, i.e. activated and, less frequently, non-activated. In case of activated chemical adsorption the rate varies with the temperature (in accordance with the Arrhenius equation) requiring a finite activation energy ranging between 8.4 and 83.7 kJ/mol [24].

The entropy and enthalpy of activation are evaluated [25] by the Eyring equation (Eq. 8):

$$ln(k_2/T) = ln(k_b/h) + (\Delta S^* /R) – (\Delta H^*/RT) \qquad (8)$$

where k_2 is the rate constant, k_b is the Boltzmann constant (J/K), h is the Planck's constant (J/s), ΔH^* is the enthalpy of activation (kJ/mol), while ΔS^* is the entropy of activation (J/mol K). The enthalpy of activation, ΔH^*, is calculated from the slope ($-\Delta H/R$) of the linear dependence of $ln(k_2/T)$ versus $1/T$ (Fig. 7), whereas the entropy of activation, ΔS^*, is calculated from the corresponding intercept $[ln(k_b/h) + (\Delta S^*/R)]$. The free energy of activation is presented by:
$$\Delta G^* = \Delta H^* – T \Delta S^* \qquad (9)$$
The values of ΔH^* and ΔS^* of the adsorption process are equal to -11.98 kJ/mol and 85.06 J/molK, respectively. The obtained thermodynamic parameter values, including the energy of activation, suggest that chemisorption dominates Ni(II) adsorption on BFS. The negative value of the enthalpy indicates the exothermic nature of the adsorption process. The positive ΔS^* value corresponds to an increase of the degrees of freedom at the solid–liquid interface during the process studied verifying the ion-exchange adsorption mechanism [26]. The ΔG^* values ($-36,90$ kJ/mol) are found negative indicating in turn that the adsorption process is spontaneous and thermodynamically favorable.

CONCLUSIONS

The kinetic parameters obtained show that the adsorption of dissolved nickel ions on BFS proceeds in accordance with a pseudo-second order model. It is clear that the mechanism of Ni(II) ions adsorption on BFS involves complex processes including outer (film-diffusion) and intra-particle diffusions. The value of the activation enthalpy verifies the exothermic character of the process. The negative activation free energy

confirms the spontaneity of the adsorption process. The thermodynamic parameter values and that of the activation energy suggest that chemisorption dominates Ni(II) adsorption on BFS.

It can be concluded that BFS may be used for nickel ions removal by the simple batch procedure. It acts as an alternative to more costly adsorbents.

REFERENCES

1. M. Ahmaruzzaman, Industrial wastes as low-cost potential adsorbents for the treatment of wastewater laden with heavy metals, Adv. Colloid. Interfac., 166, 2011, 36-59.
2. S. Malamis, E. Katsou, A review on zinc and nickel adsorption on natural and modified zeolite, bentonite and vermiculite: Examination of process parameters, kinetics and isotherms, J. Hazard. Mater., 252-253, 2013, 428-461.
3. A. Rađenović, J. Malina, A. Štrkalj, Removal of Ni(II) from aqueous solution by low-cost adsorbents, The Holistic Approach to Environment, 1, 2011, 109-120.
4. V.K. Gupta, I. Ali, Environmental Water: Advances in treatment, remediation and recycling, Elsevier, Amsterdam, 2013.
5. B. Das, S. Prakash, P.S.R. Reddy, V.N. Misra, An overview of utilization of slag and sludge from steel industries, Resour. Conserv. Recy., 50, 2007, 40-57.
6. A. Štrkalj, A. Rađenović, J. Malina, Use of waste anode dust for sorption of Ni(II) from aqueous solution, Can. Metall. Quart., 50, 2011, 3-9.
7. A. Rađenović, G. Medunić, T. Sofilić, The use of ladle furnace slag for the removal of hexavalent chromium from an aqueous solution, Metall. Res. Technol., 113, 2016, 606-617.
8. A. Bhatnagar, M. Sillanpää, Utilization of agro-industrial and municipal waste materials as potential adsorbents for water treatment—A review, Chem. Eng. J., 157, 2010, 277-296.
9. J. Malina, A. Rađenović, Kinetic Aspects of Methylene Blue Adsorption on Blast Furnace Sludge, Chem. Biochem. Eng. Q., 28, 2014, 491-498.
10. J. Fries, H. Getros, Organic reagents for trace analysis, E. Merck, Darmstadt, 1977.
11. R.C. Bansal, J.B. Donnet, F. Stoeckli, Active carbon, Marcel Dekker, New York, 1988.
12. K.K. Singh, R. Rastogi, S.H. Hasan, Removal of cadmium from wastewater using agricultural waste 'rice polish'', J. Hazard. Mater., A121, 2005, 51-58.
13. K. Chaithanya, S. Yedla, Adsorption of hexa-valent chromium using treated wood charcoal – elucidation of rate-limiting process, Environ. Technol., 31, 2010, 1495-1505.
14. C. Balan, I. Volf, D. Bilba, Chromium (VI) removal from aqueous solutions by purolite base anion-exchange resins with gel structure, Chem. Ind. Chem. Eng. Q., 19, 2013, 615-628.
15. S. Lagergren, About the theory of so-called adsorption of soluble substances, Kungliga Svenska Vetenskapsakademiens Handlingar, 24, 1898, 1-39.
16. G. McKay, Y.S. Ho, Pseudo-second order model for sorption processes, Process. Biochem., 34, 1999, 451-465.
17. W.J.Jr. Weber, J.C. Morris, Kinetics of adsorption on carbon from solution, J. Sanit. Eng. Div., 89, 1963, 31-59.
18. Y.S. Ho, G. McKay, Sorption of dyes and copper ions onto biosorbents, Process. Biochem., 38, 2003, 1047-1061.
19. K.V. Kumar, K. Porkodi, Equilibrium, kinetics and mechanism modeling and simulation of basic and acid dyes sorption onto jute fiber carbon: Eosin yellow, malachite green and crystal violet single component systems, J. Hazard. Mater., 146, 2007, 214-226.
20. P. Vassileva, A. Detcheva, I. Uzunov, S. Uzunova, Removal of metal ions from aqueous solutions using pyrolyzed rice husks: adsorption kinetics and equilibria, Chem. Eng. Commun., 200, 2013, 1578-1599.
21. G.E. Boyd, A.M. Adamson, L.S. Myers, The exchange adsorption of ions from aqueous solutions by organic zeolites. III. Performance of deep adsorbent beds under non-equilibrium conditions, J. Am. Chem. Soc., 69, 1947, 2836-2848.
22. D.J. Reichenberg, Properties of ion-exchange resins in relation to their structure. III. Kinetics of exchange, Am. Chem. Soc., 75, 1953, 589-597.
23. P. Atkins, J. De Paula, Physical Chemistry, WH Freeman and Comp., Oxford, 2006.
24. Z. Aksu, Determination of the equilibrium, kinetic and thermodynamic parameters of the batch biosorption of nickel (II) ions onto Chlorella vulgaris, Process. Biochem., 38, 2002, 89-99.

25. A.F. Holleman, E. Wiberg, Inorganic Chemistry, Academic Press, San Diego, 2001.
26. S. Chen, Q. Yue, B.Gao, X. Xu, Equilibrium and kinetic adsorption study of the adsorptive removal of Cr (VI) using modified wheat residue, J. Colloid. Interf. Sci., 349, 2010, 256-264.